Carbon Trends 4 (2021) 100077

Contents lists available at ScienceDirect

Carbon Trends

journal homepage: www.elsevier.com/locate/cartre

Single material thermocouples from graphite traces: Fabricating extremely simple and low cost thermal sensors

Rafiq Mulla, Charles W. Dunnill*

Energy Safety Research Institute, Swansea University, Bay Campus, Fabian Way, Swansea SA1 8EN, UK

ARTICLE INFO

Article history:
Received 2 May 2021
Revised 16 June 2021
Accepted 17 June 2021

Keywords:
Thermocouple
Single metal thermocouple
Graphite trace
Pencil thermocouple
Temperature sensor

ABSTRACT

Thermocouples are a universal type of thermal sensors routinely used in different applications for the measurement and monitoring of temperature. Traditionally, they are constructed from two dissimilar conductors. In this work, single material thermocouples are fabricated using graphite pencil traces patterned on cellulose paper. The different magnitudes of the Seebeck coefficients in different grade pencils facilitate successful construction of a graphite-only thermocouple sensor. These extremely simple, low-cost, and eco-friendly thermocouple sensors have shown stable and reliable sensitivity of 7.4 (±0.3) μVK^{-1}, indicating a good temperature resolution of better than 0.2 K. With the advantage of simple and solvent-free fabrication process, such devices can be developed as cheap, environmentally friendly, and disposable thermal sensors.

1. Introduction

Thermocouples are essentially simple devices but extremely useful and widely deployed for temperature measurement and monitoring tools, being used in a broad range of scientific and industrial environments [1]. In a standard structure, a thermocouple is made up of two conductors/metals that are joined together to form a measuring junction. Use of two dissimilar conductors having different Seebeck coefficients (S=$\Delta V/\Delta T$; ΔV is the voltage produced along a conductor due to the temperature gradient, ΔT) is essential to build a thermocouple, as it works on the principle of Seebeck effect. When the junction of a thermocouple is heated, a detectable open circuit voltage (V_{oc}) can be observed according to the following [1-3]:

$$V_{oc} = (S_1 - S_2)\Delta T \quad (1)$$

Where S_1 and S_2 are the Seebeck coefficients of conductor 1 and 2, respectively. The generation of a net voltage across the circuit is due to different voltage development along the two conductors resulting from the temperature difference between the hot junction and the cold junction (Fig. 1). If both the conductors are the same or have equal Seebeck coefficients then there can be no detectable voltage from the thermocouple sensor thus in theory, it is not possible to build a thermocouple from a single conductor. Interestingly, researchers have developed single metal thermocouples by a nanoscale approach [1, 4-8]. These nanoscale thermocouples are produced from two thin strips of a single metal with cross-sectional discontinuity or different strip widths in which the Seebeck coefficients become different due to size effects. In such designs, a detectable open circuit voltage is achieved by fabricating one of the strips with nanoscale width, as the changes in the Seebeck coefficients can be seen by significantly decreasing the material dimensions. For illustration, a previous work on a Ni thin film based single metal thermocouple with strip widths of 100 μm and 3 μm has reported a maximum sensitivity of 1.1 μV K^{-1}[4]. Similarly, in a Pd thin film based single metal thermocouple with dual strips of widths 30 μm and 200 nm, a thermal sensitivity of 2.2 μV K^{-1} has been achieved [7]. Very recently, high sensitivity of 39 μV K^{-1} has been observed in a graphene based thermocouple having strip widths of 1.2 μm and 0.2 μm [5].

In this work, a new and low-cost "single material thermocouple" (SMT) formation is demonstrated using graphite pencil traces on cellulose paper. The variation in the magnitude of the Seebeck coefficients in different grade pencils facilitates the successful construction of a graphite-only thermocouple without the need of nanoscale approach that in general requires special fabrication facilities. These simple designs show good thermal sensitivity of 7.4 μV K^{-1} signifying their potential as low-cost single conductor thermal sensors.

* Corresponding author.
E-mail address: c.dunnill@swansea.ac.uk (C.W. Dunnill).

https://doi.org/10.1016/j.cartre.2021.100077

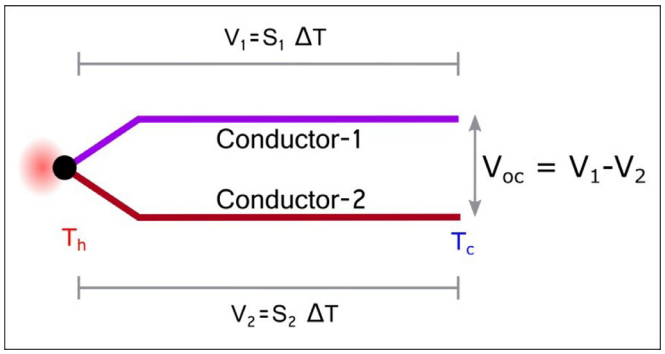

Fig. 1. Schematic of a conventional thermocouple (V_1 and V_2 are the Seebeck voltages generated along the conductor 1 and 2, respectively).

As there is a growing demand for fast and accessible information, disposable sensors are becoming increasingly important [9]. The presented graphite trace on paper based sensors can be used as disposable sensors as they are low-cost, nontoxic and easy to use. Furthermore, cellulose paper is an attractive material for disposable sensors owing to its inexpensive, lightweight, flexible and biodegradable properties [9]. In addition, as it is well known, the thermoelectric generators can directly convert thermal gradients into useful electric potential using the Seebeck effect [10]. They can be more productive in transforming waste heat into electrical energy. However, the current commercial devices are largely fabricated from expensive and toxic inorganic materials, many of which are even scarce [11-13].

Alternatively, carbon based compounds such as simple graphite traces/films or carbon/polymer based nontoxic composites can be utilized for application in order to fabricate cost-effective and flexible thermoelectric devices [14-19]. Many carbon materials have shown promising thermoelectric properties, in particular, carbon nanotubes [20, 21], carbon fibres [22-24], and graphene [25-27] have shown good Seebeck coefficient and electrical properties [26]. Recent studies demonstrated the use of carbon materials can be more beneficial to produce composites. Some polymer/organic-carbon and inorganic-carbon composites are reported with improved thermoelectric performances [19, 26, 28-31]. Also, in bulk graphite and its composites useful thermoelectric properties are observed [16, 17, 32-34].

2. Experimental section

2.1. Materials

Different grade (HB, 2B, 4B, 5B, 6B) graphite pencils (WH-Smith) were used to produce graphite traces/patterns and commonly available office Xerox paper (80 g m^{-2}) was used as a platform for constructing graphite based thermocouple junctions.

2.2. Seebeck coefficient and electrical conductivity measurements

Rectangular pencil traces of length 10 mm and width 4 mm (Fig. 2) were created on paper for the initial thermoelectric measurements. For each pencil trace, the output voltage or Seebeck voltage (ΔV) along the trace was measured as a function of applied temperature gradient (ΔT) between the hot and cold sides of the trace using a lab-built apparatus [35]. The measurement setup is schematically illustrated in Figure S1 (*Supporting Information*). In a typical measurement, samples were mounted between two thin Cu electrodes using silver conductive paint. The Cu electrodes with built-in heaters (resistive heaters) and k-type thermocouples were utilized to generate temperature difference and read temperatures at either end of the sample, respectively. The Cu wires connected to the electrodes used to read the output voltage of the samples under an applied temperature difference. Temperatures were controlled by varying the power input to the heaters and readings were obtained after reaching stabilized temperatures. About 4–6 °C temperature difference was applied along the length of the samples and average values of Seebeck coefficient were estimated from the standard expression [36, 37]:

$$S = -\left(\frac{\Delta V}{\Delta T}\right) \tag{2}$$

Measurements were carried out under a closed chamber to avoid fluctuations in the temperature and the output voltage readings, and the top side of the sample was covered with a high temperature polyimide adhesive tape (act as a thermally and electrically insulating layer) to minimize air contact with the sample, as illustrated in Figure S1 (*Supporting Information*).

Electrical conductivity measurements performed with the four probe method. A setup of four linear and equidistant point probes (spring loaded, gold coated copper probes with pointed ends), with a probe separation of 2.5 mm used for the purpose. Small currents (I = 10–50 μA) were passed through the outer two probes and the resulting voltage (V) from the sample was measured using inner probes. The resistivity (ρ) of the sample was obtained using the standard expression [38],

$$\rho = \frac{V}{I} 2\pi d \tag{3}$$

where d is the distance between the probes. The above obtained values divided with a correction factor, $g=(2d/t)$ ln2 [38], to obtain the actual resistivity of the samples, where t is the thickness of the graphite trace. The need for a correction factor is due to the proximity of a sample's boundary which limits the possible current paths during the measurements. The resistivity formula in Eq. (3) is used for the large samples. A thin film sample would restrict the current paths available due to its finite thickness and therefore requires a correction factor [39]. The thickness of the samples obtained from cross-sectional scanning electron microscopy, as shown in Figure S2 (*Supporting Information*) were used to estimate ρ. Measurements repeated at different positions to confirm reproducibility and find the measurement uncertainty values. Finally, electrical conductivity (σ) values obtained from the inverse values of ρ.

2.3. Fabrication of thermocouple

As shown by Fig. 3, a V-shaped graphite trace consisting of a HB and a 6B pencil trace was formed on paper to obtain a graphite-based single material thermocouple (SMT). To obtain this thermocouple device, first, a HB pencil trace (width ~4 mm, length ~4 cm) was hand-drawn on paper and then a 6B pencil trace (width ~4 mm, length ~4 cm) was created with one of its ends to overlap on one end of the HB pencil trace which forms a junction, as illustrated in Figure S3 (*Supporting Information*).

A paper strip SMT was fabricated by drawing pencil traces (width ~4 mm, length ~4 cm) on either side of a small paper strip. The traces were shorted at one end of the strip using a carbon conducting paste and copper foils were connected to the other ends of the pencil traces to read output voltages. The paper strip sensor was then covered with polyimide tape (high temperature tape) to protect the pencil traces and to improve the sensor's lifetime upon repeated use. Fig. 5 shows a schematic cross-sectional view and a real image of the paper strip SMT. The morphologies of the pencil traces on paper were obtained by Scanning Electron Microscopy (SEM) using Zeiss Evo LS25 SEM. Raman spectroscopy was carried out on a Renishaw inVia Raman Microscope and X-ray

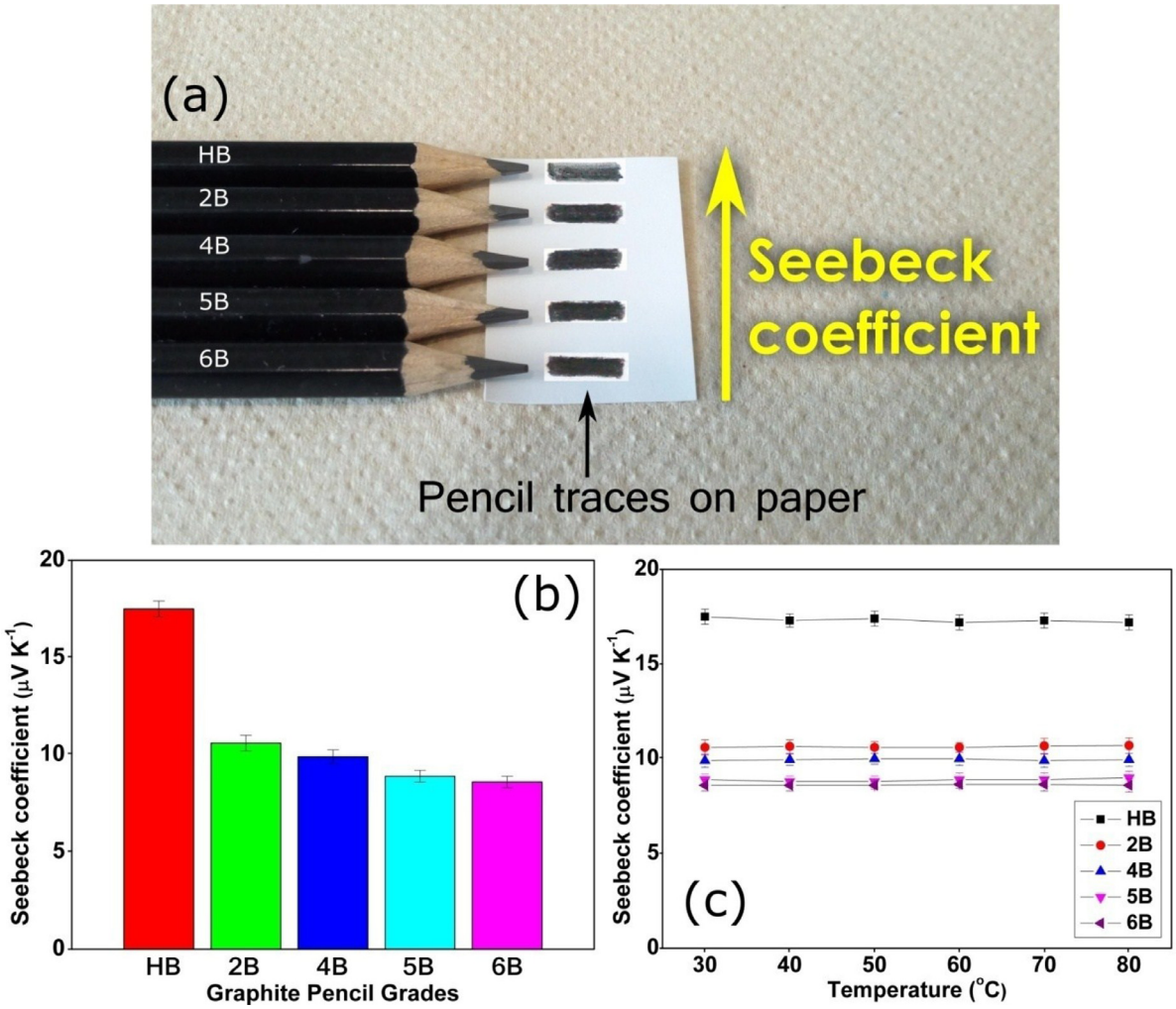

Fig. 2. (a) An illustration showing variation of the Seebeck coefficient in different grade pencil traces, (b) measured room-temperature Seebeck coefficient of different pencil traces, and (c) temperature-dependent Seebeck coefficient of the traces.

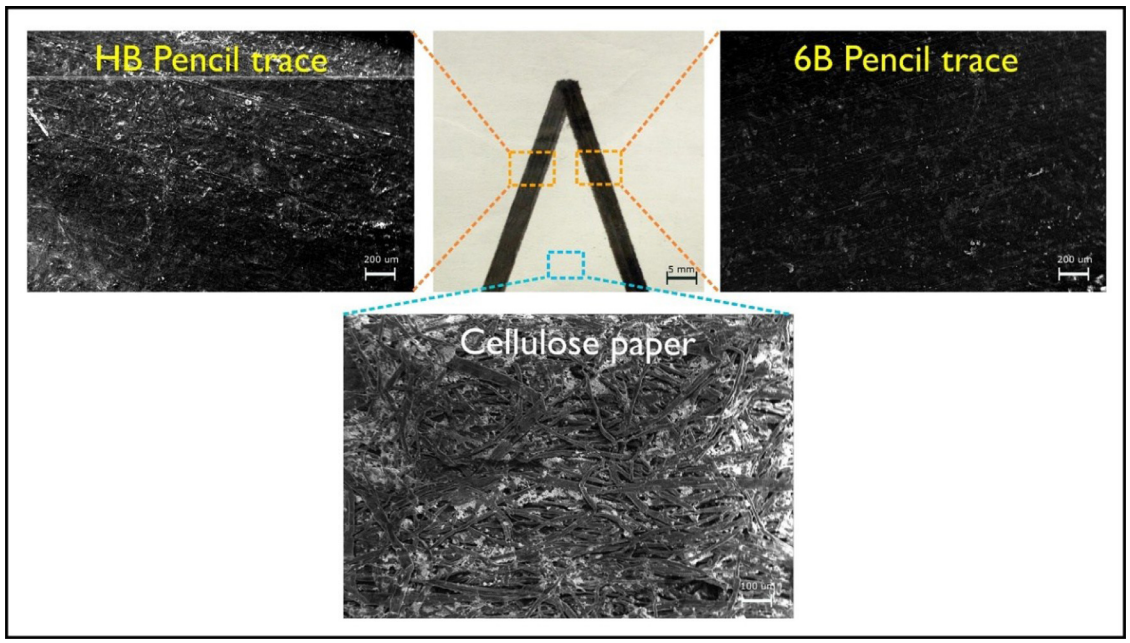

Fig. 3. Scanning electron microscopy (SEM) images of the HB and 6B pencil traces on paper that form a thermocouple sensor, along with SEM image of bare cellulose paper substrate.

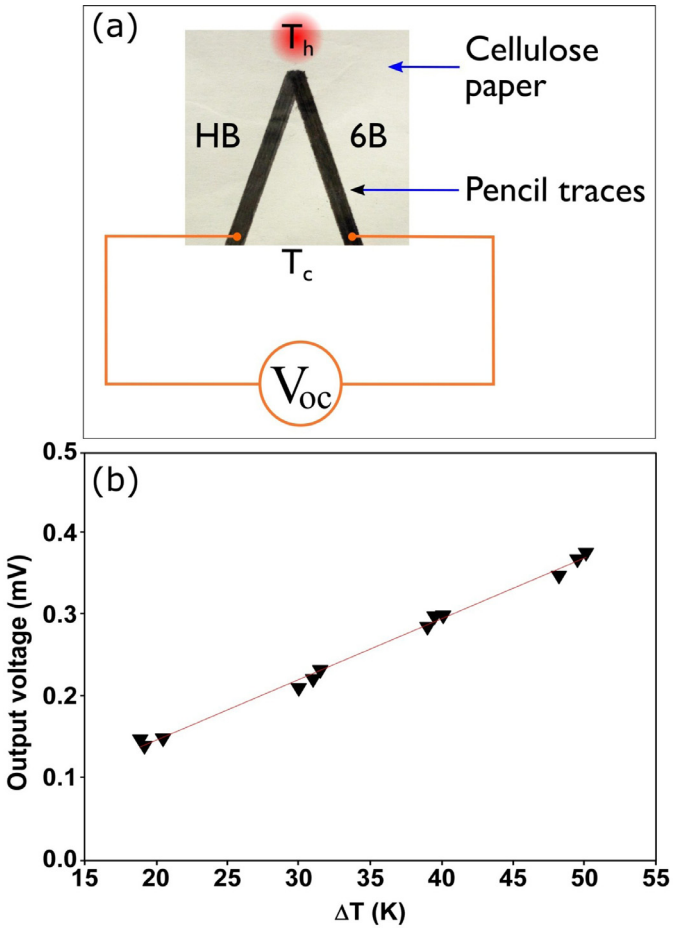

Fig. 4. (a) A V-shaped single material thermocouple (SMT) formed by using HB and 6B pencil traces, and (b) its output voltage data at different temperature gradients (ΔT).

diffraction (XRD) patterns of the samples were acquired through use of a Bruker D8 diffractometers.

2.4. Fabrication of multiple junction thermocouples

Multiple junction thermocouple patterns having four measuring junctions were fabricated using HB and 6B pencil traces (trace width ~2 mm) with HB trace as a common lead for all four junctions (Fig. 7 and Fig. 8). Copper electrical contacts were connected to read outputs from the trace leads.

2.5. Testing of thermocouple devices

The output voltage measurements of the as-fabricated SMT devices carried out with a labmade platform in open conditions at room temperature (~295 K) [40]. The junction of a thermocouple heated to different temperatures to achieve different temperature gradients between the junction and cold ends and recorded resulting output voltages from the device. To test the working of multiple junction SMT devices, a small resistive heater was used to achieve local heating in order to observe the variations in the output voltages from the thermocouples. Digital multimeters of voltage resolution 1 μV (Model: HMC 8012 DMM) used for all the measurements. Measurements repeated 4–5 times to confirm the reproducibility of the data.

3. Results and discussion

Commercially available pencils, ranging from HB to 6B were employed to construct a graphite based single material thermocouple (SMT). The difference between the Seebeck coefficients (thermopower) of the two conducting patterns/traces of a thermocouple is a key parameter that determines its output characteristics. In order to select two suitable pencil grades to construct an SMT, the Seebeck coefficient of all the pencil traces were first examined. Fig. 2b shows the room temperature Seebeck coefficient values of all the pencil grades. The HB grade pencil trace has shown a maximum value of 17.5 μV K^{-1} and found to decrease with changing pencil grades from HB to 6B and the lowest value of 8.6 μV K^{-1} observed in the case of 6B trace, as schematically pictured in Fig. 2a. Further, we performed temperature dependent measurements to observe the variations in the Seebeck values. As shown by Fig. 2c, increasing the temperature up to 80 °C had a negligible effect on the magnitudes of all the traces. The observed Seebeck coefficient values are consistent with previously reported values for bulk graphite or thick reduced graphene oxide (rGO) films but are smaller as compared to the reported values for graphene/few layer graphene [25-27, 41-45] carbon nanotubes, and carbon fibres [20-22, 46-50]. As the graphite traces produced on paper substrates are sufficiently thick (few microns)[15] in nature, it is logical to assume that these are bulk graphite films. Typical Seebeck values observed in thick rGO films are in the range of 10–30 μV K^{-1} (however, some studies have reported high Seebeck values when rGO is partially reduced and such high values are attributed to the presence of oxygen related functional groups in the rGO) [51] and in case of graphite, it is about 8–20 μV K^{-1} [16, 34, 42, 49, 52].

The minimum dependence of the Seebeck coefficient on temperature is a key advantage to form a thermocouple with good linearity in the output voltage signal with respect to temperature. The pencil grade dependent variation in the Seebeck coefficient of graphite traces attributed to the compositional variations in the pencil leads. Different grade pencil leads contain different levels of clay binders in graphite [53]. Generally, the amount of clay binders decreases from HB to 6B grade. For illustration, a typical HB pencil contains 68% graphite, 26% clay, 5% wax, whereas a 6B pencil contains 84% graphite, 10% clay, 5% wax [53]. Table S1 (*Supporting Information*) shows the amount of graphite in different grade graphite pencils. These clay binders expected to play an important role in changing the electrical properties of the resulting graphite traces. The electrical conductivity (σ) of pencil traces shown in Figure S4 (*Supporting Information*) increases from HB to 6B grade trace which is due to the increasing graphite content in the pencils. The measured values are in near agreement with the previous studies on the electrical conductivity of different grade graphite pencil traces [54]. It is well known that the Seebeck coefficient, in most cases, decreases with the increase in carrier concentration. As the electrical conductivity is directly related to the number of carriers in the material, according to $\sigma = ne\mu$ (where n, e, μ are the number, charge, and mobility of carriers), the Seebeck coefficient is expected to decrease with an increase in electrical conductivity.

A good adherence property of graphitic particles of the pencil on cellulose paper substrates helps create desired conductive patterns and circuits with simple pencil hand-drawing, which are shown to be promising in low-cost and flexible electronics such as sensors [55-59], energy storage devices [60-67], resistors [68], transistors [69], and also in thermoelectric applications [14, 15]. To illustrate the morphology of the as deposited graphitic layers/flakes on cellulose paper, SEM images of the pencil traces on paper are shown in Fig. 3. The traces covered the cellulose fibres of the paper and resulted in a continuous graphitic film. Further, X-ray diffraction patterns of HB and 6B traces shown in Figure S5 (*Supporting Information*) confirm that the formed traces on paper are graphite

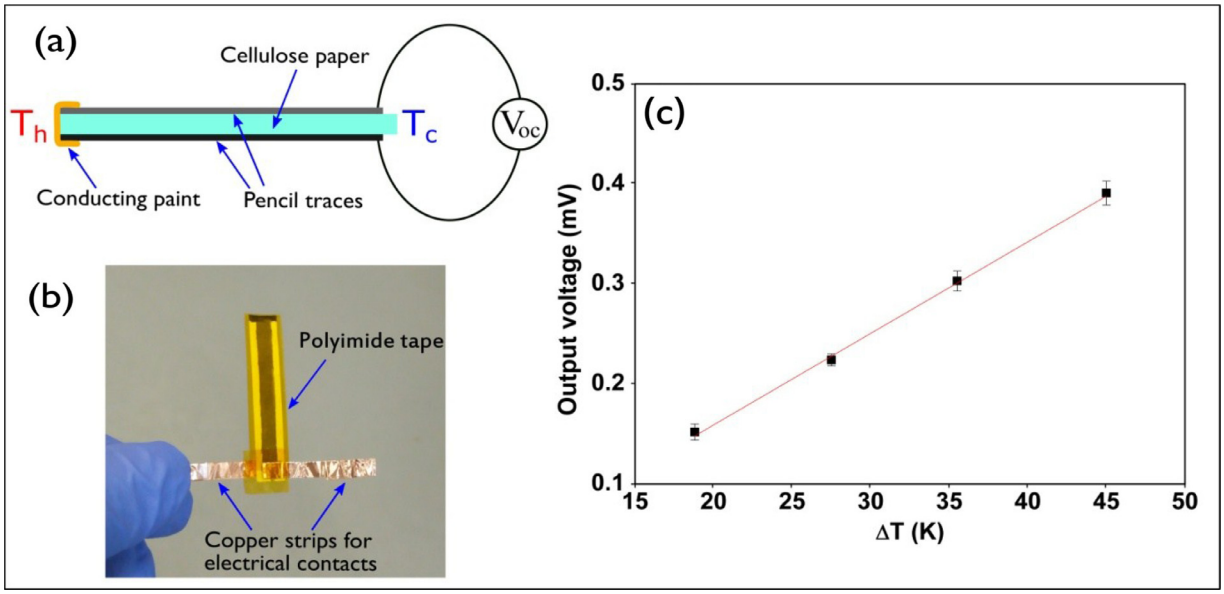

Fig. 5. (a) Cross-sectional and (b) a real image of a single conductor thermocouple (SMT) on a small paper strip, and (c) its output characteristics at different temperature gradients (ΔT).

films. The samples show a prominent peak at 26.6° related to (002) plane of graphite (JCPDS file 41–1487), indicating preferred orientation along (002) crystallographic direction and the intensity of the peak illustrates that the graphite traces formed on paper have good crystallinity. The higher intensity peak of (002) plane in 6B trace as compared to HB trace expected to be associated with the more graphite content in it, as also observed in previous works [70]. The minor peak at 29.3° can be assigned to the calcite ($CaCO_3$) compound present in the paper substrate [71]. Figure S6 (*Supporting Information*) shows the Raman spectra of graphite pencil traces. All the patterns show the expected Raman signatures for graphite, with prominent peaks at ~1330 cm^{-1} (D band) and ~1580 cm^{-1} (G band) [72]. The G bands of all the samples exhibit a shoulder at ~1615 cm^{-1} (D' band), typical of defective graphite materials [72]. The lattice disorder of graphite is typically evaluated from the ratio of D band to G band intensity (I_D/I_G) [73]. The I_D/I_G ratios of HB, 2B, 4B, 5B, and 6B graphite traces are 0.62, 0.60, 0.51, 0.49, and 0.54, respectively, indicating a higher degree of disorder in HB and 2B samples as compared to others. The different levels of clay binders present in these samples could be responsible for the changes in the I_D/I_G ratios.

A maximum difference in the Seebeck coefficient can be obtained from the combination of HB and 6B pencil traces thus are used to design and fabricate thermocouple devices. A simple SMT displayed in Fig. 4a has two strips (HB and 6B traces) that join to form a junction. The open-circuit voltage (ΔV) as a function of temperature gradient (ΔT) presented in Fig. 4b shows an excellent linear curve in the measured range of ΔT of up to 50 K, indicating a constant sensitivity of the sensor with a slope value of 7.4 (±0.3) μV K^{-1}. The output voltage data align well with linear fittings with an R^2 value of 0.996. An improved design of the above SMT sensor is shown in Fig. 5 along with its output characteristics. It is found to be a more convenient and standard structure of the sensor that can be formed out of a small paper strip. Here also, the ΔV data were similar to the previous version with excellent linearity as a function of ΔT. With such a good thermal sensitivity of more than 7 μV K^{-1}, these graphite trace based SMT can measure temperatures with resolution better than 0.2 K with a micro-voltmeter (Note: As the micro-voltmeter can measure a minimum value of 1 μV, the present device with a sensitivity of 7 μV K^{-1} can provide a temperature resolution of 1 μV / 7 μV K^{-1} = 0.14 K, or approximately "better than 0.2 K".) Better resolutions in the temperatures can be realized with high resolution voltmeters. The sensitivity of these graphite based devices can further be enhanced with additional dopants [14]. For example, some organic/polymer compounds have properties that successfully change the Seebeck coefficients of graphite [14, 15]. Therefore, improved Seebeck values can help fabricate devices with better sensitivity.

Alongside, the thermal sensing response of these graphite sensors is reasonably fast. The variation in the output voltage signal of the sensor when it was brought in contact with a hot object was recorded as a function of time, illustrated in Figure S7 (*Supporting Information*) which demonstrates quick thermal sensing of the sensor.

To further confirm the dissimilar Seebeck effects in HB and 6B pencil traces, a two junction pattern is formed by inserting the first conductor (HB trace) between two sections of a second conductor (6B trace) forming two junctions, as depicted in Fig. 6a. When these two junctions (1 and 2) are at different temperatures, the circuit should produce a non-zero output voltage. Alongside, a change in the polarity of the output voltage is expected when the hot junction is reversed. To observe this effect, a pre-heated hot metal block was placed on junction-1 which produced a positive voltage signal (Fig. 6b). A sudden fall in the voltage signal was observed upon removing the hot block. Next, a pre-heated hot block of the same temperature as used earlier was placed on junction-2 that successfully produced a negative voltage signal as expected, confirming the change in the direction of charge flow between the junctions due to the change of the hot junction from junction-1 to junction-2.

As these graphite trace based thermocouple sensors can be easily patterned on paper substrates, a reliable and low-cost temperature mapping of a specific length or area can be achieved with multiple junction design. A simple structure of a multiple junction sensor is shown in Fig. 7 where HB trace (lead-3) was used as a common lead for all four junctions (A, B, C, D) located at different positions. Such designs are convenient to use and reduce the number of output contacts from the sensors. To test its working, the multiple sensor pattern was placed below a thin glass slide (0.5 mm) and a small resistive heater was placed close to junction-

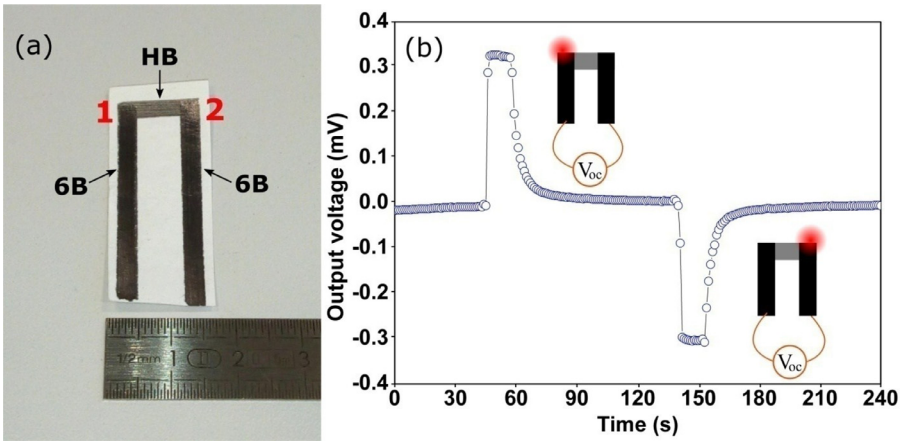

Fig. 6. (a) Graphite trace pattern fabricated from HB and 6B traces to study signal generation by creating temperature gradient between junctions 1 and 2, and (b) its output voltage signal.

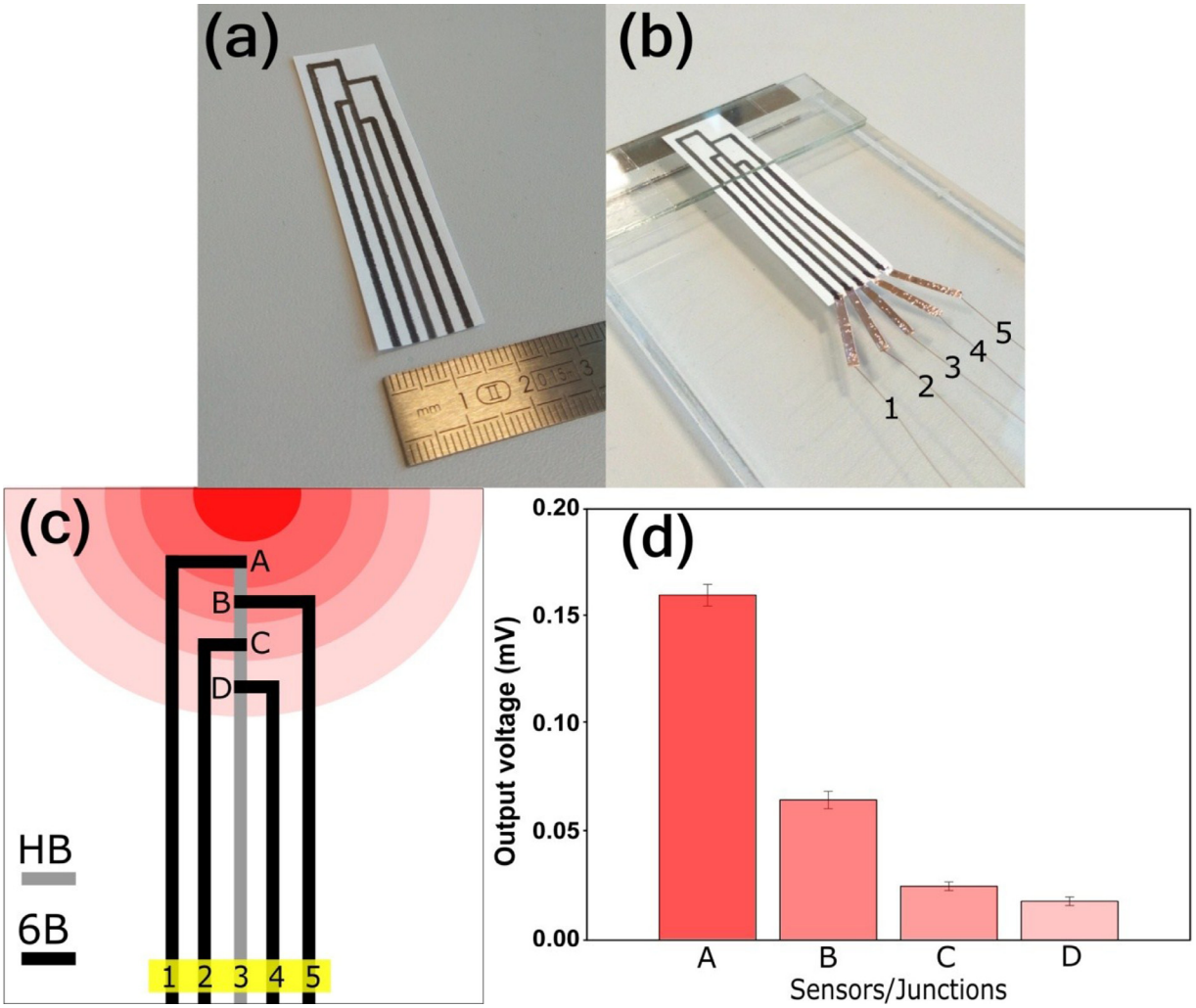

Fig. 7. (a-b) Images of multiple thermocouple sensor for temperature mapping, (c) its schematic illustrating temperature field, and (d) voltage output of multiple sensors (Junctions-A, B, C, D) where heater was located near junction-A. (lead 3 is a HB trace that act as a common lead for all four sensors, leads 1, 2, 4, and 5 are 6B traces).

A and turned on to generate a thermal field on the surface, as illustrated by the color pattern in Fig. 7c. The temperature sensing is different at different junctions as they are at different distances from the heater. The output signals observed from the sensors are plotted in Fig. 7d. Other possible designs of multiple junctions are illustrated in Fig. 8a. A real picture of as-fabricated multiple sensors (similar to Design-1) is displayed in Fig. 8b and output voltage signal data of the sensors as a function of heater location are shown in Fig. 8c. Also, the variation in the output signals from the sensors is recorded as a function of time after the heater (placed near Junction-A) is turned ON (the data is shown in Figure S8 (*Supporting Information*)). Further, the observed data was reproducible,

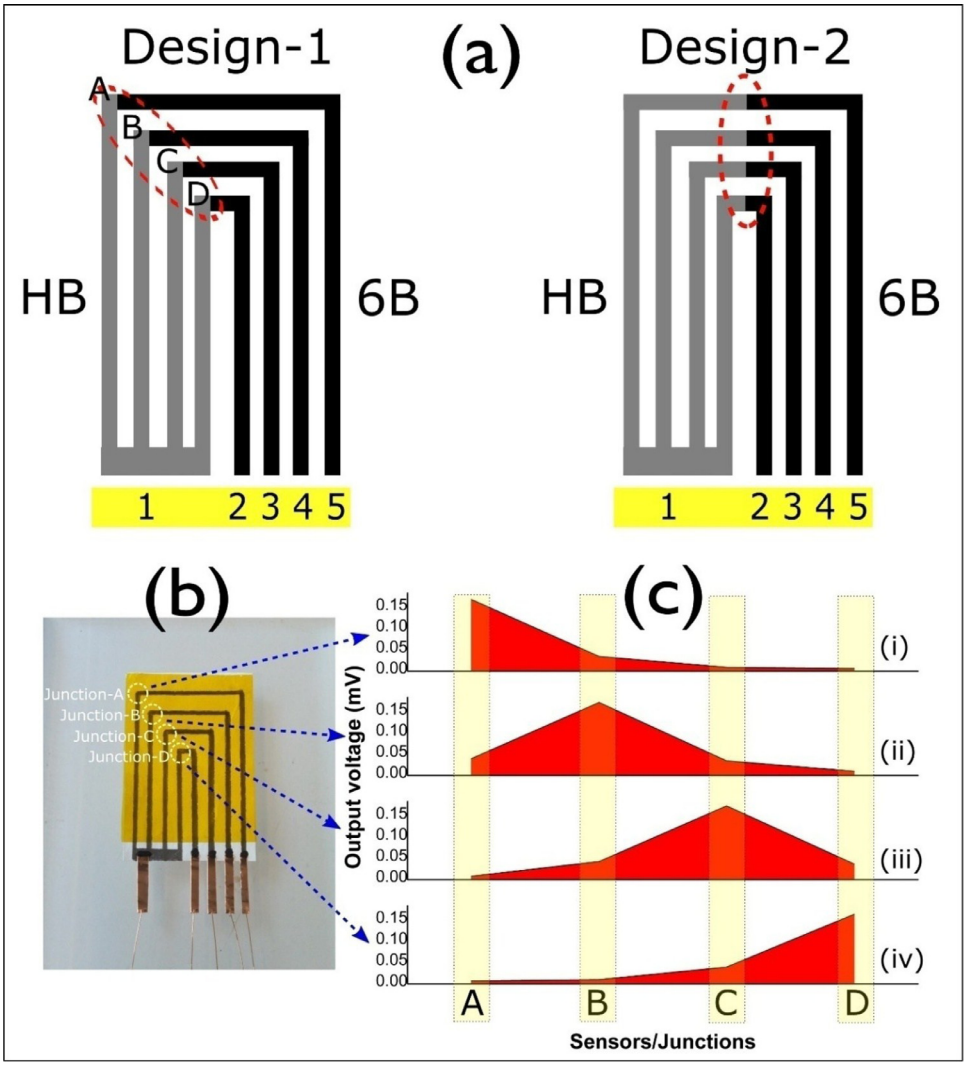

Fig. 8. (a) Designs of multiple thermocouple sensor for temperature mapping, (b) a real picture of a sensor, and (c) output voltage data of the sensors as a function of heater location. The voltage data in graphs (i), (ii), (iii), and (iv) are recorded with heater located at junction-A, B, C, and D respectively (lead 1 is a HB trace that act as a common lead for all four sensors, leads 2, 3, 4, and 5 are 6B traces).

the magnitude of data scatter in the output signal of the multiple sensors when the heater was located at junction-A is shown in Figure S9 (*Supporting Information*) as a representative. The results of these measurements indicate that these simple graphite sensors patterned on paper strips can also be utilized for time-resolved mapping of local temperatures of a given surface. With proper improvements in the design and substrates, these type of disposable thermal sensors may be utilized in a range of applications such as (i) cold storage delivery of things like vaccines, medicines, and food, (ii) temperature sensitive deliveries, (iii) medical applications with disposable thermal sensor patches for measuring fever in patients [74, 75], (iv) lab-on-a-chip immunosensors [76] or biosensors [77] and many others [78, 79].

4. Conclusions

Extremely simple thermal sensors in the form of pencil traces on paper have been fabricated and demonstrated as “single material thermocouples” (SMTs). These sensors show a good and stable thermal sensitivity of 7.4 (±0.3) μV K^{-1}, indicating a temperature resolution of better than 0.2 K. The merits of simple structure and reliable performance can make these graphite trace patterns as promising sensors for temperature sensing. In addition, with such a simple and solvent-free fabrication process, these pencil trace based devices can be developed as cheap, environmentally friendly, and disposable thermal sensors.

Data availability

Data that support the findings are available in the supplementary information of the manuscript.

Declaration of Competing Interest

The authors declare no conflict of interest.

Acknowledgments

Authors are thankful to the Welsh Government (EU European Regional Development Fund) for funding the RICE (Reducing Industrial Carbon Emission) project (Grant Number: 81435). Authors would like to acknowledge the assistance provided by Swansea University College of Engineering AIM Facility, which was funded in part by the EPSRC (EP/M028267/1), the European Regional Development Fund through the Welsh Government (80708) and the Ser Solar project via Welsh Government.

Supplementary materials

Supplementary material associated with this article can be found, in the online version, at doi:10.1016/j.cartre.2021.100077.

References

[1] G.P. Szakmany, A.O. Orlov, G.H. Bernstein, W. Porod, Single-metal nanoscale thermocouples, IEEE Trans. Nanotechnol. 13 (6) (2014) 1234–1239.
[2] W. Sun, H. Liu, W. Gong, L.-.M. Peng, S.-.Y. Xu, Unexpected size effect in the thermopower of thin-film stripes, J. Appl. Phys. 110 (8) (2011) 083709.
[3] H. Liu, W. Sun, A. Xiang, T. Shi, Q. Chen, S. Xu, Towards on-chip time-resolved thermal mapping with micro-/nanosensor arrays, Nanoscale Res. Lett. 7 (1) (2012) 484.
[4] H. Liu, W. Sun, S. Xu, An extremely simple thermocouple made of a single layer of metal, Adv. Mater. 24 (24) (2012) 3275–3279.
[5] A. Harzheim, F. Könemann, B. Gotsmann, H. van der Zant, P. Gehring, Single–material graphene thermocouples, Adv. Funct. Mater. 30 (22) (2020) 2000574.
[6] G.P. Szakmany, A.O. Orlov, G.H. Bernstein, W. Porod, Polarization-dependent response of antenna-coupled single-metal thermocouples, in: 2014 Silicon Nanoelectronics Workshop (SNW), 2014, pp. 1–2.
[7] X. Huo, H. Liu, Y. Liang, M. Fu, W. Sun, Q. Chen, S. Xu, A nano-stripe based sensor for temperature measurement at the submicrometer and nano scales, Small 10 (19) (2014) 3869–3875.
[8] X. Huo, J. Xu, Z. Wang, F. Yang, S. Xu, Performance of nano-submicron-stripe Pd thin-film temperature sensors, Nanoscale Res. Lett. 11 (1) (2016) 351.
[9] C. Dincer, R. Bruch, E. Costa-Rama, M.T. Fernández-Abedul, A. Merkoçi, A. Manz, G.A. Urban, F. Güder, Disposable sensors in diagnostics, food, and environmental monitoring, Adv. Mater. 31 (30) (2019) 1806739.
[10] Y. Wang, L. Yang, X.-.L. Shi, X. Shi, L. Chen, M.S. Dargusch, J. Zou, Z.-.G. Chen, Flexible thermoelectric materials and generators: challenges and innovations, Adv. Mater. 31 (29) (2019) 1807916.
[11] R. Mulla, C.W. Dunnill, Powering the hydrogen economy from waste heat: a review of heat-to-hydrogen concepts, ChemSusChem 12 (17) (2019) 3882–3895.
[12] R. Mulla, D.R. Jones, C.W. Dunnill, Economical and facile route to produce gram-scale and phase-selective copper sulfides for thermoelectric applications, ACS Sustain. Chem. Eng. 8 (37) (2020) 14234–14242.
[13] R. Mulla, M.H.K. Rabinal, Copper sulfides: earth-abundant and low-cost thermoelectric materials, Energy Technol. 7 (7) (2019) 1800850.
[14] V.V. Brus, M. Gluba, J. Rappich, F. Lang, P.D. Maryanchuk, N.H. Nickel, Fine art of thermoelectricity, ACS Appl. Mater. Interfaces 10 (5) (2018) 4737–4742.
[15] R. Mulla, D.R. Jones, C.W. Dunnill, Thermoelectric paper: graphite pencil traces on paper to fabricate a thermoelectric generator, Adv. Mater. Technol. 5 (7) (2020) 2000227.
[16] R. Mulla, C.W. Dunnill, Graphite-loaded cotton wool: a green route to highly–porous and solid graphite pellets for thermoelectric devices, Comp. Commun. 20 (2020) 100345.
[17] Y. Du, H. Li, X. Jia, Y. Dou, J. Xu, P. Eklund, Preparation and thermoelectric properties of graphite/poly(3,4-ethyenedioxythiophene) nanocomposites, Energies 11 (10) (2018) 2849.
[18] Y.-.Y. Hsieh, Y. Zhang, L. Zhang, Y. Fang, S.N. Kanakaraaj, J.-.H. Bahk, V. Shanov, High thermoelectric power-factor composites based on flexible three-dimensional graphene and polyaniline, Nanoscale 11 (14) (2019) 6552–6560.
[19] L. Wang, Q. Yao, H. Bi, F. Huang, Q. Wang, L. Chen, PANI/graphene nanocomposite films with high thermoelectric properties by enhanced molecular ordering, J. Mater. Chem. A 3 (13) (2015) 7086–7092.
[20] J.L. Blackburn, A.J. Ferguson, C. Cho, J.C. Grunlan, Carbon-nanotube-based thermoelectric materials and devices, Adv. Mater. 30 (11) (2018) 1704386.
[21] D. Abol-Fotouh, B. Dörling, O. Zapata-Arteaga, X. Rodríguez-Martínez, A. Gómez, J.S. Reparaz, A. Laromaine, A. Roig, M. Campoy-Quiles, Farming thermoelectric paper, Energy Environ. Sci. 12 (2) (2019) 716–726.
[22] G. Karalis, L. Tzounis, E. Lambrou, L.N. Gergidis, A.S. Paipetis, A carbon fiber thermoelectric generator integrated as a lamina within an 8-ply laminate epoxy composite: efficient thermal energy harvesting by advanced structural materials, Appl. Energy 253 (2019) 113512.
[23] W.-.Y. Chen, X.-.L. Shi, J. Zou, Z.-.G. Chen, Wearable fiber-based thermoelectrics from materials to applications, Nano Energy 81 (2021) 105684.
[24] A.J. Paleo, E.M.F. Vieira, K. Wan, O. Bondarchuk, M.F. Cerqueira, L.M. Goncalves, E. Bilotti, P. Alpuim, A.M. Rocha, Negative thermoelectric power of melt mixed vapor grown carbon nanofiber polypropylene composites, Carbon N Y 150 (2019) 408–416.
[25] N.S. Sankeshwar, S.S. Kubakaddi, B.G. Mulimani, Thermoelectric power in graphene, Advances in Graphene Science in: M. Aliofkhazraei (Ed.), IntechOpen, 2013.
[26] P.-a. Zong, J. Liang, P. Zhang, C. Wan, Y. Wang, K. Koumoto, Graphene-based thermoelectrics, ACS Appl. Energy Mater. 3 (3) (2020) 2224–2239.
[27] T.G. Novak, J. Kim, J. Kim, A.P. Tiwari, H. Shin, J.Y. Song, S. Jeon, Complementary n-type and p-type graphene films for high power factor thermoelectric generators, Adv. Funct. Mater. 30 (28) (2020) 2001760.
[28] X. Chen, H. Zhang, Y. Zhao, W.-.D. Liu, W. Dai, T. Wu, X. Lu, C. Wu, W. Luo, Y. Fan, L. Wang, W. Jiang, Z.-.G. Chen, J. Yang, Carbon-encapsulated copper sulfide leading to enhanced thermoelectric properties, ACS Appl. Mater. Interfaces 11 (25) (2019) 22457–22463.
[29] A. Bhardwaj, A.K. Shukla, S.R. Dhakate, D.K. Misra, Graphene boosts thermoelectric performance of a Zintl phase compound, RSC Adv. 5 (15) (2015) 11058–11070.
[30] B. Feng, J. Xie, G. Cao, T. Zhu, X. Zhao, Enhanced thermoelectric properties of p-type CoSb3/graphene nanocomposite, J. Mater. Chem. A 1 (42) (2013) 13111–13119.
[31] L. Huang, J. Lu, D. Ma, C. Ma, B. Zhang, H. Wang, G. Wang, D.H. Gregory, X. Zhou, G. Han, Facile in situ solution synthesis of SnSe/rGO nanocomposites with enhanced thermoelectric performance, J. Mater. Chem. A 8 (3) (2020) 1394–1402.
[32] P. Singha, S. Das, V.A. Kulbachinskii, V.G. Kytin, A.S. Apreleva, D.J. Voneshen, T. Guidi, A.V. Powell, S. Chatterjee, A.K. Deb, S. Bandyopadhyay, A. Banerjee, Evidence of improvement in thermoelectric parameters of n-type Bi2Te3/graphite nanocomposite, J. Appl. Phys. 129 (5) (2021) 055108.
[33] V. Andrei, K. Bethke, K. Rademann, Adjusting the thermoelectric properties of copper(i) oxide–graphite–polymer pastes and the applications of such flexible composites, PCCP 18 (16) (2016) 10700–10707.
[34] J. Li, L. Wang, X. Jia, X. Xiang, C.-.L. Ho, W.-.Y. Wong, H. Li, Preparation and thermoelectric properties of diphenylaminobenzylidene-substituted poly(3-methylthiophene methine)/graphite composite, RSC Adv. 4 (107) (2014) 62096–62104.
[35] R. Mulla, M.K. Rabinal, A simple and portable setup for thermopower measurements, ACS Comb Sci 18 (4) (2016) 177–181.
[36] K.A. Borup, J. de Boor, H. Wang, F. Drymiotis, F. Gascoin, X. Shi, L. Chen, M.I. Fedorov, E. Müller, B.B. Iversen, G.J. Snyder, Measuring thermoelectric transport properties of materials, Energy Environ. Sci. 8 (2) (2015) 423–435.
[37] R. Mulla, M.K. Rabinal, A tweezer as a thermoelectric tester, Phys. Educ. 54 (5) (2019) 055032.
[38] Y. Singh, Electrical resistivity measurements: a review, Int. J. Modern Phys. 22 (2013) 745–756.
[39] L. Valdes, Resistivity measurements on germanium for transistors, Proc. IRE 42 (2) (1954) 420–427.
[40] R. Mulla, K. Glover, C.W. Dunnill, An easily constructed and inexpensive tool to evaluate the seebeck coefficient, IEEE Trans. Instrum. Meas. 70 (2021) 1–7.
[41] A.S. Nissimagoudar, N.S. Sankeshwar, Electronic thermal conductivity and thermopower of armchair graphene nanoribbons, Carbon N Y 52 (2013) 201–208.
[42] T.G. Novak, J. Kim, J. Kim, H. Shin, A.P. Tiwari, J.Y. Song, S. Jeon, Flexible thermoelectric films with high power factor made of non-oxidized graphene flakes, 2D Materials 6 (4) (2019) 045019.
[43] J.H. Seol, I. Jo, A.L. Moore, L. Lindsay, Z.H. Aitken, M.T. Pettes, X. Li, Z. Yao, R. Huang, D. Broido, N. Mingo, R.S. Ruoff, L. Shi, Two-dimensional phonon transport in supported graphene, Science 328 (5975) (2010) 213.
[44] X. Li, J. Yin, J. Zhou, Q. Wang, W. Guo, Exceptional high Seebeck coefficient and gas-flow-induced voltage in multilayer graphene, Appl. Phys. Lett. 100 (18) (2012) 183108.
[45] S.S. Kubakaddi, Giant thermopower and power factor in magic angle twisted bilayer graphene at low temperature, J. Phys. Condens. Matter 33 (24) (2021) 245704, doi:10.1088/1361-648X/abf0c2.
[46] A.D. Avery, B.H. Zhou, J. Lee, E.-.S. Lee, E.M. Miller, R. Ihly, D. Wesenberg, K.S. Mistry, S.L. Guillot, B.L. Zink, Y.-.H. Kim, J.L. Blackburn, A.J. Ferguson, Tailored semiconducting carbon nanotube networks with enhanced thermoelectric properties, Nature Energy 1 (4) (2016) 16033.
[47] S. Kim, J.-.H. Mo, K.-.S. Jang, Solution-processed carbon nanotube buckypapers for foldable thermoelectric generators, ACS Appl. Mater. Interfaces 11 (39) (2019) 35675–35682.
[48] X. Li, Z. Yu, H. Zhou, F. Yang, F. Zhong, X. Mao, B. Li, H. Xin, C. Gao, L. Wang, Promoting the thermoelectric performance of single-walled carbon nanotubes by inserting discotic liquid-crystal molecules, ACS Sustain. Chem. Eng. 9 (4) (2021) 1891–1898.
[49] Z. Fan, Y. Zhang, L. Pan, J. Ouyang, Q. Zhang, Recent developments in flexible thermoelectrics: from materials to devices, Renew. Sustain. Energy Rev. 137 (2021) 110448.
[50] J. Fan, X. Huang, F. Liu, L. Deng, G. Chen, Feasibility of using chemically exfoliated SnSe nanobelts in constructing flexible SWCNTs-based composite films for high-performance thermoelectric applications, Composites Commun. 24 (2021) 100612.
[51] J. Choi, N.D.K. Tu, S.-.S. Lee, H. Lee, J.S. Kim, H. Kim, Controlled oxidation level of reduced graphene oxides and its effect on thermoelectric properties, Macromol. Res. 22 (10) (2014) 1104–1108.
[52] N.D.K. Tu, J.A. Lim, H. Kim, A mechanistic study on the carrier properties of nitrogen-doped graphene derivatives using thermoelectric effect, Carbon N Y 117 (2017) 447–453.
[53] M.C. Sousa, J.W. Buchanan, Observational Models of Graphite Pencil Materials, Comput. Graphics Forum 19 (1) (2000) 27–49.
[54] H. Zhao, T. Zhang, R. Qi, J. Dai, S. Liu, T. Fei, Drawn on paper: a reproducible humidity sensitive device by handwriting, ACS Appl. Mater. Interfaces 9 (33) (2017) 28002–28009.
[55] T.-.L. Ren, H. Tian, D. Xie, Y. Yang, Flexible graphite-on-paper piezoresistive sensors, Sensors 12 (5) (2012).
[56] K. ul Hasan, O. Nur, M. Willander, Screen printed ZnO ultraviolet photoconductive sensor on pencil drawn circuitry over paper, Appl. Phys. Lett. 100 (21) (2012) 211104.
[57] Z. Li, H. Liu, X. He, F. Xu, F. Li, Pen-on-paper strategies for point-of-care testing of human health, TrAC Trends Anal. Chem. 108 (2018) 50–64.
[58] C.-.W. Lin, Z. Zhao, J. Kim, J. Huang, Pencil drawn strain gauges and chemiresistors on paper, Sci. Rep. 4 (1) (2014) 3812.

[59] C. Wang, K. Xia, H. Wang, X. Liang, Z. Yin, Y. Zhang, Advanced carbon for flexible and wearable electronics, Adv. Mater. 31 (9) (2019) 1801072.
[60] Y. Wang, H. Zhou, To draw an air electrode of a Li–air battery by pencil, Energy Environ. Sci. 4 (5) (2011) 1704–1707.
[61] Y. Yu, J. Zhang, Pencil-drawing assembly to prepare graphite/MWNT hybrids for high performance integrated paper supercapacitors, J. Mater. Chem. A 5 (9) (2017) 4719–4725.
[62] S. Zhu, Y. Li, H. Zhu, J. Ni, Y. Li, Pencil-drawing skin-mountable micro-supercapacitors, Small 15 (3) (2019) 1804037.
[63] Z. Tai, Y. Liu, Q. Zhang, T. Zhou, Z. Guo, H.K. Liu, S.X. Dou, Ultra-light and flexible pencil-trace anode for high performance potassium-ion and lithium-ion batteries, Green Energy Environment 2 (3) (2017) 278–284.
[64] S.H. Lee, J.Y. Ban, C.-.H. Oh, H.-.K. Park, S. Choi, A solvent-free microbial-activated air cathode battery paper platform made with pencil-traced graphite electrodes, Sci. Rep. 6 (1) (2016) 28588.
[65] H.-.Y. Park, M.-.S. Kim, T.-.S. Bae, J. Yuan, J.-.S. Yu, Fabrication of Binder-Free Pencil-Trace Electrode for Lithium-Ion Battery: simplicity and High Performance, Langmuir 32 (18) (2016) 4415–4423.
[66] L. Zhang, X. Qin, S. Zhao, A. Wang, J. Luo, Z.L. Wang, F. Kang, Z. Lin, B. Li, Advanced matrixes for binder-free nanostructured electrodes in lithium-ion batteries, Adv. Mater. 32 (24) (2020) 1908445.
[67] P. Rani, K.S. Kumar, A.D. Pathak, C.S. Sharma, Pyrolyzed pencil graphite coated cellulose paper as an interlayer: an effective approach for high-performance lithium-sulfur battery, Appl. Surf. Sci. 533 (2020) 147483.
[68] N. Kurra, G.U. Kulkarni, Pencil-on-paper: electronic devices, Lab Chip 13 (15) (2013) 2866–2873.
[69] N. Kurra, D. Dutta, G.U. Kulkarni, Field effect transistors and RC filters from pencil-trace on paper, PCCP 15 (21) (2013) 8367–8372.
[70] J. Kim, D. Ahn, J. Sun, S. Park, Y. Cho, S. Park, S. Ha, S. Ahn, Y.A. Kim, J.-.J. Park, Vertically and horizontally drawing formation of graphite pencil electrodes on paper by frictional sliding for a disposable and foldable electronic device, ACS Omega 6 (3) (2021) 1960–1970.
[71] A.C. Marques, L. Santos, M.N. Costa, J.M. Dantas, P. Duarte, A. Gonçalves, R. Martins, C.A. Salgueiro, E. Fortunato, Office paper platform for bioelectrochromic detection of electrochemically active bacteria using tungsten trioxide nanoprobes, Sci. Rep. 5 (1) (2015) 9910.
[72] D.A. Bradley, Z. Siti Rozaila, M.U. Khandaker, K.S. Almugren, W. Meevasana, S.F. Abdul Sani, Raman spectroscopy and X-ray photo-spectroscopy analysis of graphite media irradiated at low doses, Appl. Radiat. Isot. 147 (2019) 105–112.
[73] Z.-.S. Wu, W. Ren, L. Gao, J. Zhao, Z. Chen, B. Liu, D. Tang, B. Yu, C. Jiang, H.-.M. Cheng, Synthesis of graphene sheets with high electrical conductivity and good thermal stability by hydrogen arc discharge exfoliation, ACS Nano 3 (2) (2009) 411–417.
[74] Y. Su, C. Ma, J. Chen, H. Wu, W. Luo, Y. Peng, Z. Luo, L. Li, Y. Tan, O.M. Omisore, Z. Zhu, L. Wang, H. Li, Printable, highly sensitive flexible temperature sensors for human body temperature monitoring: a review, Nanoscale Res. Lett. 15 (1) (2020) 200.
[75] A.J. Wang, S. Maharjan, K.-.S. Liao, B.P. McElhenny, K.D. Wright, E.P. Dillon, R. Neupane, Z. Zhu, S. Chen, A.R. Barron, O.K. Varghese, J. Bao, S.A. Curran, Poly(octadecyl acrylate)-grafted multiwalled carbon nanotube composites for wearable temperature sensors, ACS Appl. Nano Mater. 3 (3) (2020) 2288–2301.
[76] S.M.I. Bari, L.G. Reis, G.G. Nestorova, Calorimetric sandwich-type immunosensor for quantification of TNF-α, Biosens. Bioelectron. 126 (2019) 82–87.
[77] G.G. Nestorova, B.S. Adapa, V.L. Kopparthy, E.J. Guilbeau, Lab-on-a-chip thermoelectric DNA biosensor for label-free detection of nucleic acid sequences, Sens. Actuators B 225 (2016) 174–180.
[78] G.G. Nestorova, V.L. Kopparthy, N.D. Crews, E.J. Guilbeau, Thermoelectric lab-on-a-chip ELISA, Anal. Methods 7 (5) (2015) 2055–2063.
[79] Y. Xu, G. Zhao, L. Zhu, Q. Fei, Z. Zhang, Z. Chen, F. An, Y. Chen, Y. Ling, P. Guo, S. Ding, G. Huang, P.-.Y. Chen, Q. Cao, Z. Yan, Pencil–paper on-skin electronics, Proc. Natl. Acad. Sci. 117 (31) (2020) 18292.